Different mechanisms for phytoalexin induction by pathogen and wound signals in *Medicago truncatula*

Marina Naoumkina*, Mohamed A. Farag*†, Lloyd W. Sumner*, Yuhong Tang*, Chang-Jun Liu‡, and Richard A. Dixon*§

*Plant Biology Division, Samuel Roberts Noble Foundation, 2510 Sam Noble Parkway, Ardmore, OK 73401, †Department of Pharmacognosy, Faculty of Pharmacy, Cairo University, Kasr El Aini Street, Cairo, Egypt; and ‡Department of Biology, Brookhaven National Laboratory, Upton, NY 11973

This contribution is part of the special series of Inaugural Articles by members of the National Academy of Sciences elected on May 1, 2007.

Contributed by Richard A. Dixon, September 13, 2007 (sent for review July 1, 2007)

Cell suspensions of the model legume *Medicago truncatula* accumulated the isoflavonoid phytoalexin medicarpin in response to yeast elicitor or methyl jasmonate (MJ), accompanied by decreased levels of isoflavone glycosides in MJ-treated cells. DNA microarray analysis revealed rapid, massive induction of early (iso)flavonoid pathway gene transcripts in response to yeast elicitor, but not MJ, and differential induction by the two elicitors of sets of genes encoding transcription factors, ABC transporters, and β-glucosidases. In contrast, both elicitors induced genes encoding enzymes for conversion of the isoflavone formononetin to medicarpin. Four MJ-induced β-glucosidases were expressed as recombinant enzymes in yeast, and three were active with isoflavone glucosides. The most highly induced β-glucosidase was nuclear localized and preferred flavones to isoflavones. The results indicate that the genetic and biochemical mechanisms underlying accumulation of medicarpin differ depending on the nature of the stimulus and suggest a role for MJ as a signal for rapid hydrolysis of preformed, conjugated intermediates for antimicrobial biosynthesis during wound responses.

glucosidase | methyl jasmonate | phytoanticipin | cell culture | elicitation

Many plant natural products have antimicrobial or antiinsect activity *in vitro*, and genetically reducing or increasing levels of certain natural products can reduce or enhance resistance or tolerance to microbes or pests (1–3). Antimicrobial plant natural products have been classified as phytoanticipins, which are preformed inhibitory compounds, or phytoalexins, which are derived from often distant precursors via *de novo* synthesis in response to microbial challenge (4).

Consistent with *de novo* synthesis of phytoalexins, many studies have documented rapid activation of their diverse biosynthetic genes in response to fungal or bacterial infection of plant organs or treatment of plant cell cultures with microbial-derived elicitor molecules (5–7). However, some reports fail to demonstrate a link between phytoalexin accumulation and increased transcription of related biosynthetic genes (e.g., ref. 8). Utilization of additional approaches such as determination of metabolite levels and/or enzymatic activities might help explain the rare cases in which phytoalexin induction is observed in the apparent absence of changes at the transcriptional level.

Some natural products, for example, isoflavonoids and triterpenes, show activity against both microbial and insect challengers of the plants that produce them (9–11). Root-derived cell suspension lines of the model legume *Medicago truncatula* studied previously accumulated the isoflavonoid-derived pterocarpan phytoalexin medicarpin in response to treatment with yeast elicitor (YE), and triterpene saponins after exposure to the wound signal methyl jasmonate (MJ) (12–14). To investigate the different molecular mechanisms underlying metabolic responses to pathogen and wound signals, we have used an integrated transcriptome/metabolome analysis of a different root-derived *Medicago* cell suspension culture line that accumulates medicarpin in response to both YE and MJ. This culture was of the same genotype (A17) as the previously studied cultures and was propagated under the same conditions (13), the only differences being the independent initial root explant and the passage number at which the experiments were performed. Surprisingly, transcript profiling analysis revealed that none of the genes encoding early enzymes of phenylpropanoid/isoflavonoid biosynthesis was induced before accumulation of medicarpin in response to MJ in this culture line, although the downstream pathway genes specific for medicarpin formation were induced by both treatments. MJ-inducible β-glucosidases were functionally characterized and shown to be active with (iso)flavonoid glycosides and therefore potentially involved in precursor mobilization for medicarpin biosynthesis. Our results suggest that MJ acts as a signal for the rapid deployment of preexisting intermediates into phytoalexin biosynthesis during wound responses.

Results

Metabolic Responses to YE or MJ. Exposure of *M. truncatula* cells to YE resulted in a 15-fold increase in medicarpin levels, accompanied by increases in the levels of the intermediates isoliquiritigenein and liquiritigenin; smaller increases in the levels of the glycosides of the isoflavones daidzein, genistein, biochanin A, and formononetin were also observed [Fig. 1 and supporting information (SI) Fig. 6]. The chemical identifications of the *Medicago* (iso)flavonoids are described elsewhere (14), and further details of the temporal changes and metabolic interrelationships between the various compounds will be presented later (M.A.F., R.A.D., and L.W.S., unpublished data). In contrast, MJ induced an unexpected 36-fold increase in medicarpin, accompanied by decreased levels of glycosides and/or malonyl glycosides of the central isoflavone intermediates daidzein, formononetin, and 2′-hydroxyformononetin (Fig. 1); previous studies with a different cell culture line had not revealed significant accumulation of medicarpin in response to MJ (13).

Transcriptional Responses to YE or MJ. Two microarray formats were used for transcript profiling as a cost-benefit compromise to allow for both temporal resolution [Operon 16K 70-mer oligonucleotide *Medicago* arrays (15) for analysis of 16 time

Author contributions: M.N. and R.A.D. designed research; M.N., M.A.F., Y.T., and C.-J.L. performed research; L.W.S. contributed new reagents/analytic tools; M.N., M.A.F., L.W.S., Y.T., C.-J.L., and R.A.D. analyzed data; and R.A.D. wrote the paper.

The authors declare no conflict of interest.

Abbreviations: YE, yeast elicitor; MJ, methyl jasmonate; TC, tentative consensus; PAL, L-phenylalanine ammonia-lyase; CHS, chalcone synthase; 2HID, 2-hydroxyisoflavanone dehydratase; CHI, chalcone isomerase; G*n*, glucosidase *n*; pNPG, *p*-nitrophenyl glucoside.

Data deposition: The sequences reported in this paper have been deposited in the GenBank database (accession nos. EU078901–EU078904).

§To whom correspondence should be addressed. E-mail: radixon@noble.org.

This article contains supporting information online at www.pnas.org/cgi/content/full/0708697104/DC1.

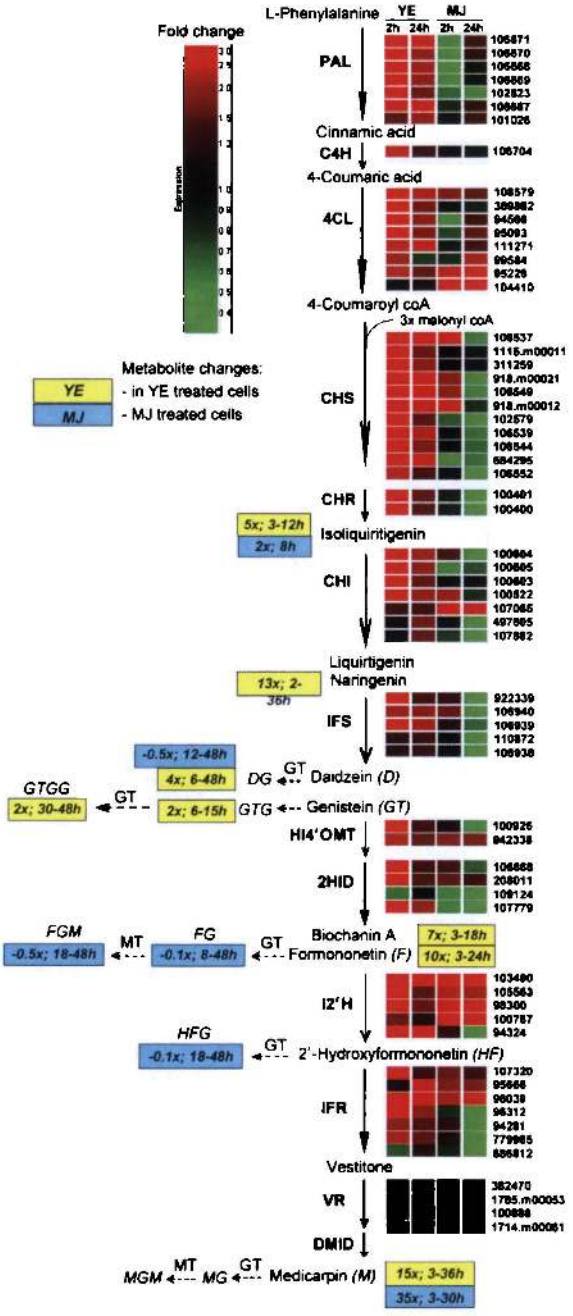

Fig. 1. Changes in medicarpin pathway transcripts and metabolites in *M. truncatula* suspension cells. Green/red color-coded heat maps represent relative transcript levels of different gene family members determined with Affymetrix arrays (red, up-regulated; green, down-regulated). Data represent ratios of expression at 2 and 24 h between treatment and control. Yellow bars show metabolite levels in YE-treated cells, and blue bars show MJ-treated cells (fold-change followed by times after elicitation during which increases or decreases occur). Abbreviations for enzyme names are given in SI Fig. 6. G, glucoside; GG, diglucoside; GM, malonyl glucoside; GT, glucosyltransferase; MT, malonyltransferase.

points up to 48 h postelicitation with YE and 11 time points after exposure to MJ] and high analytical reproducibility (Affymetrix *Medicago* arrays with >61,200 probe features) for comparing 2- and 24-h elicited samples to corresponding controls. Overall, transcriptional changes in response to YE occurred early (before 15 h after elicitation), whereas the majority of changes in the MJ-treated cultures occurred later (Fig. 2 *A* and *B*). Many of the genes up- or down-regulated by YE were also regulated by MJ (Affymetrix analysis; Fig. 2*D*); this proportion was much smaller for the oligo array analysis (Fig. 2*C*), as fewer transcripts passed the statistical analysis for elimination of false discoveries when compared with the Affymetrix data. Functional gene ontology analysis of up-regulated (SI Fig. 7 *A–D*) and down-regulated (SI Fig. 7 *E–H*) genes indicated that, overall, the responses to YE and MJ were similar.

Genes encoding transcription factors were more widely and rapidly induced by YE than by MJ (SI Fig. 7*I* and SI Table 2). Genes annotated as encoding ABC transporters were more widely induced by MJ than by YE at 24 h, although similar numbers were induced by either elicitor at 2 h. Many of the transporters up-regulated by YE were down-regulated by MJ and vice versa (SI Fig. 7*J* and SI Table 3). Among the 11 different classes of transcription factors analyzed, more members were up-regulated by YE than by MJ at 2h after elicitation, as clearly seen for the WRKY, MYB, and AP2 classes (SI Fig. 8*A*), and more were down-regulated by MJ than by YE 24 h after elicitation (SI Fig. 8*B*).

The complete Affymetrix data set is publicly available at ArrayExpresss (www.ebi.ac.uk/arrayexpress; ID = E-MEXP-1092), and the oligo array data are available at the DOME database at the Virginia Bioinformatics Institute (http://dome.vbi.vt.edu/mt).

YE, but Not MJ, Induces the Complete Medicarpin Biosynthetic Pathway. The first enzyme of the phenylpropanoid pathway, L-phenylalanine ammonia-lyase (PAL), is currently represented by at least seven different unigenes in the *M. truncatula* Gene Index (http://compbio.dfci.harvard.edu/tgi/cgi-bin/tgi/gimain.pl?gudb = medicago). Five of these genes were represented on the 16K oligo chip and were coordinately up-regulated (with maximum transcript levels at 2 h after elicitation) in response to YE (SI Fig. 9*A*). RT-PCR analysis of PAL tentative consensus (TC) 106671 confirmed this expression pattern (SI Fig. 9*B*). Five of the PAL TC contigs on the oligo chip, plus two genomic sequences, were represented on the Affymetrix array. All seven of these genes were induced by YE (Fig. 1). In contrast, none was induced by MJ, and several were repressed at 2 h after elicitation (Fig. 1 and SI Table 4). Strong, rapid induction by YE, but lack of induction by MJ, was also observed for the single cinnamate 4-hydroxylase (*C4H*) gene, five of the eight genes annotated as encoding 4-coumarate CoA ligase, two chalcone reductases, and six chalcone isomerase (CHI) or CHI-like genes (Fig. 1 and SI Fig. 9*A*). One CHI-like gene (*TC107065*) was induced by MJ but not by YE. Eleven chalcone synthase (CHS) TCs were represented on the 16K oligo array, and 14 (five of which corresponded to TCs represented on the oligo array) on the Affymetrix chip. Most were induced by YE and down-regulated by MJ (Fig. 1, SI Fig. 9*A*, and SI Table 4). CHS TCs 106544 and 106537 were selected for additional analysis by RT-PCR (SI Fig. 9 *B* and *C*). TC106537 transcripts were induced by MJ at 4 h after elicitation but then declined below control levels (SI Fig. 9*C*).

The entry point into the isoflavonoid pathway leading to formononetin exists as a metabolon comprising three enzymes: 2-hydroxyisoflavanone synthase, 2-hydroxyisoflavanone 4′-*O*-methyltransferase, and 2-hydroxyisoflavanone dehydratase (2HID) (16, 17) (SI Fig. 6). 2HID has not been functionally characterized from *Medicago*, so we performed Blast search analysis of the *Medicago* Gene Index with the 2HID sequence characterized from *Glycirrhiza echinata* (18). Four TCs were found having from 43% to 88% amino acid similarity to 2HID (SI Fig. 10), and three of the four were induced by YE (Fig. 1). None of the genes annotated as encoding any of the three enzymes for formation of formononetin from liquiritigenin was induced by MJ (Fig. 1 and SI Table 4). In contrast, many of the TCs annotated as encoding the remaining steps of medicarpin

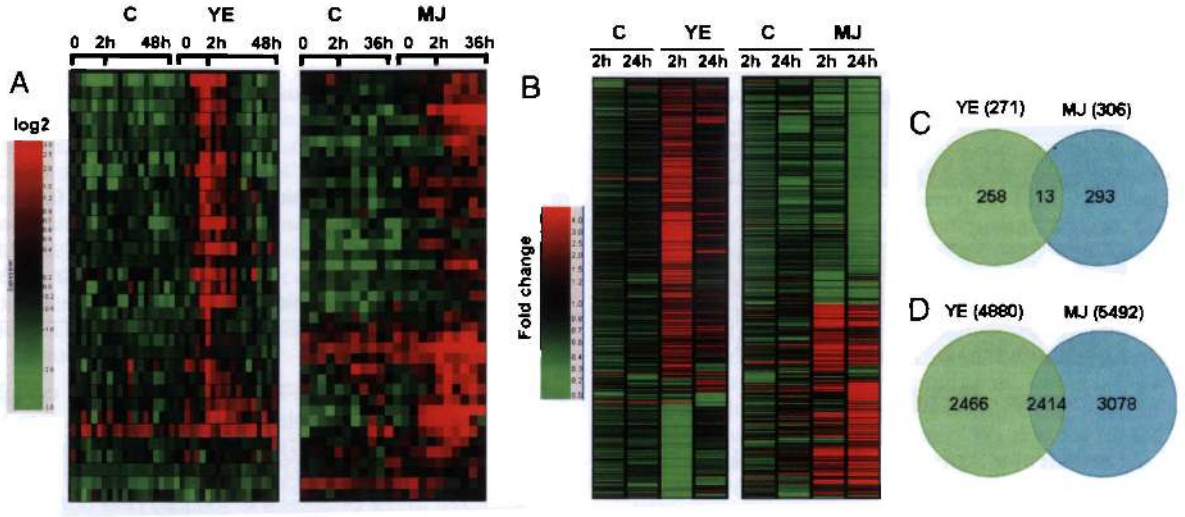

Fig. 2. Summary of global transcript changes in *M. truncatula* cell cultures exposed to YE or MJ, or in corresponding unelected controls (C). (*A*) Heat maps showing induction kinetics of 258 YE-induced genes and 293 MJ-induced genes as revealed by oligo array analysis. (*B*) Heat maps showing induction kinetics of 2,466 YE-induced genes and 3,078 MJ-induced genes as revealed by Affymetrix array analysis. (*C* and *D*) Venn diagrams showing the numbers of genes induced by YE or MJ, or genes induced by both treatments, for oligo array (*C*) and Affymetrix (*D*) analyses.

biosynthesis from formononetin (catalyzed by isoflavone 2′-hydroxylase, isoflavone reductase, and vestitone reductase) were regulated similarly by YE and MJ (Fig. 1, SI Fig. 6, and SI Table 4). Note that not all of these genes may be annotated correctly (see *Discussion*).

The differential transcriptional induction of early phenylpropanoid biosynthesis by YE might extend into supply of precursors from primary metabolism. For example, transcripts encoding enzymes of the shikimate/prephenate pathway for phenylalanine biosynthesis were generally more rapidly and strongly induced by YE than by MJ (SI Table 5), consistent with the YE-induced increase in shikimate levels in YE-treated *Medicago* cells (19).

The YE-mediated induction of a complete set of biosynthetic pathway genes for medicarpin formation involving multiple isoforms of many of the enzymes, but induction of a complete set of pathway genes only for downstream conversion of formononetin in response to MJ, highlights the significance of the MJ-induced depletion of preformed glucose conjugates of formononetin. These observations also implicate β-glucosidases in the mobilization of stored isoflavone glucosides during MJ-induced medicarpin biosynthesis.

Differential Induction of β-Glucosidases by MJ and YE. Oligo array analysis revealed four TCs annotated as encoding β-glucosidases that were induced by MJ (Fig. 3*A* and SI Fig. 9*C*), and this was confirmed by Affymetrix array analysis (Fig. 3*B*). Transcripts corresponding to TC106656 (glucosidase 1, G1) were induced by 2 h after exposure to MJ but were not induced by YE (SI Fig. 9 *C* and *D*). TC94967 (G2) was induced as early as 30 min after MJ or YE treatment, but induction was not sustained in response to YE.

Analysis of EST counts in the *M. truncatula* EST database indicated that G1 was the most highly expressed of the four glucosidases, and that all were most highly represented in cDNA libraries from root tissues [the major site of isoflavone metabolism in nonstressed *Medicago* plants (20)] or MJ-induced cell cultures (SI Fig. 11*A*). Affymetrix array analysis confirmed that expression of all four β-glucosidases was almost exclusively in root tissues, with G1 and TC107558 (G3) also weakly expressed in seeds (SI Fig. 11*B*).

Functional Analysis of *Medicago* β-Glucosidases. Phylogenetic analysis indicated that G1, G2, and G3 clustered with plant glucosyl hydrolases from both legume and nonlegume species, and that G4 was less closely related to these enzymes and more related to a β-glucosidase from wheat (SI Fig. 12). To determine the biochemical activities of the MJ-induced *Medicago* glucosidases, their ORFs were expressed in the yeast *Pischia pastoris*. Recombinant G1 and TC109932 (G4) were recovered from the soluble intracellular fraction, and G2 and G3 were recovered from the medium. We could not purify G3 and G4 by affinity chromatography, probably because of the inaccessibility of their His tag sequences. These enzymes were therefore assayed in crude yeast lysates. All four enzymes hydrolyzed the model substrate *p*-nitrophenyl glucoside (pNPG). G1 showed a preference for flavone glucosides over isoflavone glucosides (although it was active with sissotrin, the 7-*O*-glucoside of biochanin A). G3 and G4 showed similar overall activities with both classes of compounds, and G2 preferred isoflavone glucosides such as ononin (formononetin 7-*O*-glucoside) (Fig. 3 *C* and *D* and SI Fig. 13 *B–G*). Only G3 and G4 were active with flavonol and anthocyanidin 3-*O*-glucosides, and none of the enzymes could hydrolyze flavone or isoflavone 8-*C*-glucosides (SI Table 6 and SI Fig. 13). Importantly, all enzymes, except G1, were active with ononin and could therefore be involved in MJ-induced isoflavone mobilization for medicarpin biosynthesis.

Kinetic analyses were performed for G1 and G2 with pNPG and the 7-*O*-glucosides of formononetin, genistein, and apigenin. Both enzymes had high K_{cat}/K_m ratios for the artificial substrate pNPG, but the K_m values were very high. The lowest K_m was observed for G2 with genistin as substrate, and the highest K_{cat}/K_m ratio was observed for G1 with apigenin 7-*O*-glucoside (Table 1).

Subcellular Localization of *Medicago* β-Glucosidases. By computational analysis, G2 and G3 were predicted to exhibit vacuolar or extracellular localization. G4 might localize to microbodies (peroxisomes), and G1 might localize to microbodies or nucleus (SI Table 7). Modeling of G1 based on the structure of white clover (*Trifolium repens*) cyanogenic β-glucosidase (21) (with 55.6% amino acid sequence identity) revealed an unusually extended N terminus (Fig. 4*K*). This "tail" contains the sequence PPKRKRPH, characteristic of nuclear localization signals for plant proteins (22–24).

The ORFs of the four glucosidases were fused in-frame to the

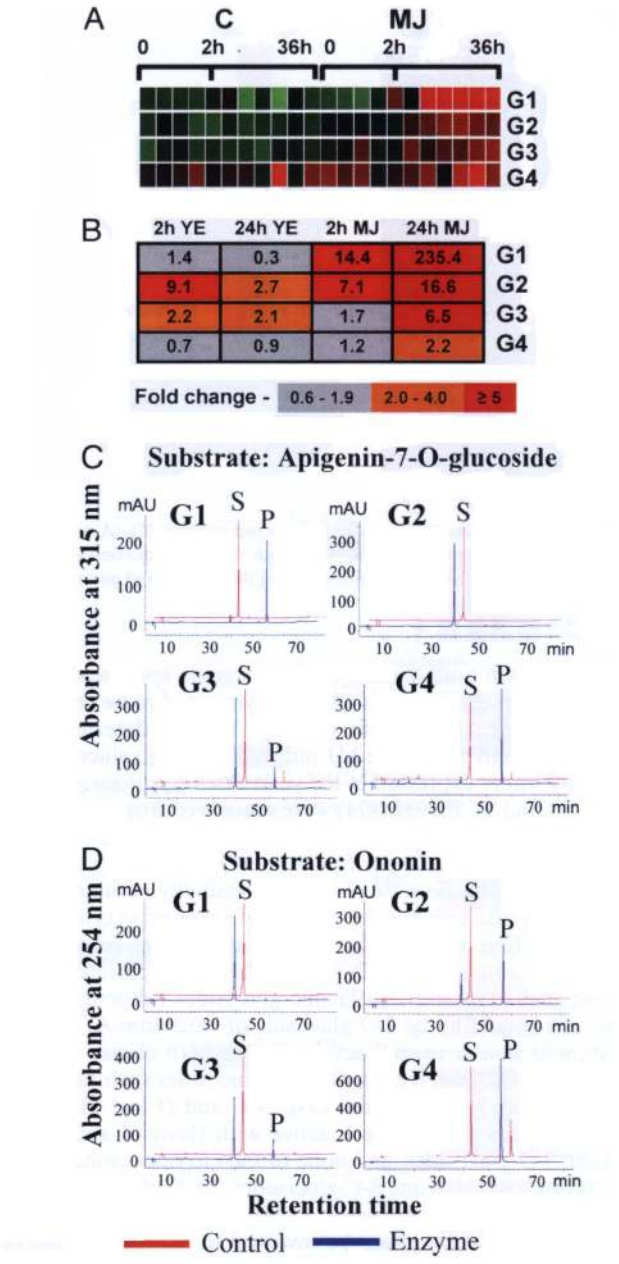

Fig. 3. Expression of β-glucosidases in *M. truncatula* cell cultures. (*A*) Induction of β-glucosidases by MJ as revealed by oligo array analysis. C, control. (*B*) Glucosidase transcript levels in YE- and MJ-elicited cultures determined by Affymetrix arrays. Values represent fold changes compared with control cultures. (*C* and *D*) HPLC chromatograms showing product formation after incubation of recombinant glucosidases with flavonoid (*C*) and isoflavonoid (*D*) substrates. s = substrate (glycoside) and p = product (corresponding aglycone). G1 and G2 were assayed with purified enzyme, G3 was assayed with extract from cell medium, and G4 was assayed with cell lysates (see *SI Text*). Controls for G3 and G4 were from cells expressing empty vector. The basal rates of hydrolysis were presumably the result of activity of endogenous *Escherichia coli* hydrolases.

EGFP reporter gene, under control of a double cauliflower mosaic virus 35S promoter. Unfortunately, no fluorescence could be recorded for G2- or G3-EGFP fusions, probably because of the instability of the fusion proteins. G1 and G4 fusion constructs were bombarded into leaves of *M. truncatula* and tobacco and into *Medicago* suspension cells (unelicited or exposed to MJ for 4 h) on agar plates. The fusions were also introduced into tobacco by

Table 1. Kinetic parameters of *Medicago* β-glucosidases

Enzyme	Substrate	V_{max}, μmol/min	K_m, μM	K_{cat}, s^{-1}	K_{cat}/K_m, s^{-1}·M^{-1}
G1	pNPG	26.5	7452	1.3	174.4
	Ononin	0	0	0	0.0
	Genistin	0	0	0	0.0
	Apigenin-7-*O*-glucoside	13.4	264.6	0.67	2,528.4
G2	pNPG	28.8	1850	3.0	1,621.6
	Ononin	5.0	126	6.7×10^{-4}	5.3
	Genistin	0.3	12.3	4×10^{-4}	32.7
	Apigenin-7-*O*-glucoside	0	0	0	0

agro-infiltration. Free EGFP accumulated in the cytoplasm and nucleus, and multiple cytoplasmic strands could be seen traversing the vacuole (Fig. 4 *A–C*). G1-EGFP localized to the nucleus in all tissues and treatments (Fig. 4 *F–I*). In contrast, EGFP fluorescence was localized to the cytoplasm in tobacco cells bombarded with a fusion from which the first 108 aa of G1 had been removed, confirming the function of the N-terminal extension of this protein

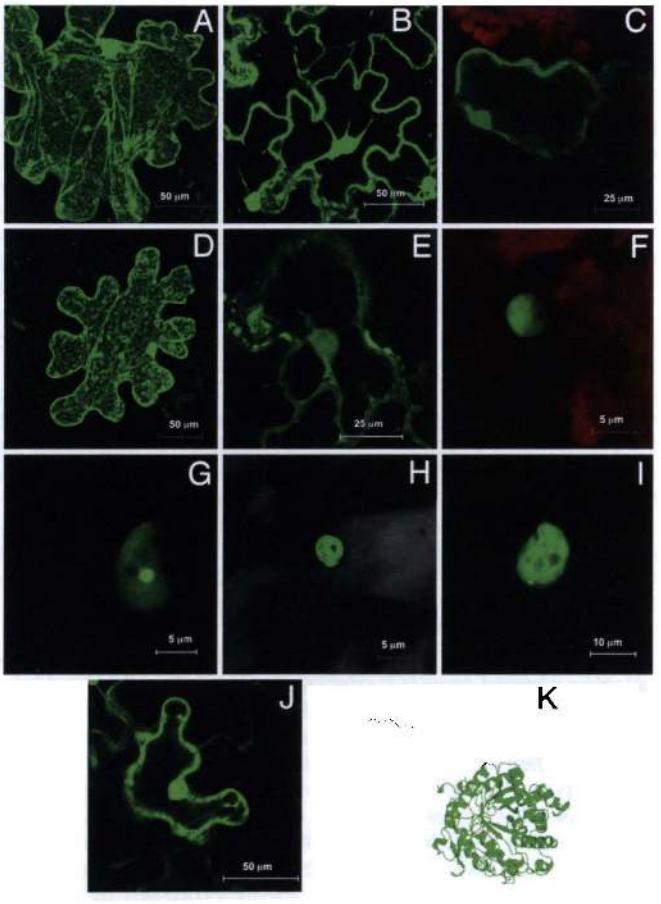

Fig. 4. Subcellular localization of *Medicago* β-glucosidases. (*A–J*) Confocal images show localization of free EGFP (*A–C*), or EGFP fused to G4 (*D* and *E*), G1 (*F–I*), or to G1 lacking 108 aa from the N terminus (*J*). Transient expression of EGFP constructs was obtained by particle bombardment of tobacco leaves (*A*, *D*, and *H*), *M. truncatula* leaves (*C* and *F*), or MJ-treated *M. truncatula* cell suspension cultures (*G*), or by agro-infiltration of tobacco leaves (*B*, *E*, *I*, and *J*). *A*, *D*, and *E* are projected stacks of Z-series, and *B*, *E*, *G*, and *I* are a single median of one confocal plane. *C* and *F* also show autofluorescence of chloroplasts. *H* is a superimposed transmitted light image onto the fluorescent image. (*K*) A ribbon model of the structure of G1, indicating the N-terminal extension and putative nuclear localization signal (in red).

for nuclear targeting (Fig. 4*J*). In contrast, G4-EGFP localized to the cytoplasm, with a similar pattern to that of free EGFP (Fig. 4 *D* and *E*).

In view of the unexpected localization of G1, we analyzed the nuclear fractions from *M. truncatula* roots for the presence of (iso)flavonoids (we were repeatedly unable to obtain intact nuclei from cell cultures). Coumestrol and 4′,7-dihydroxyflavone (as the free aglycones) were the only (iso)flavonoid compounds present in nuclei. Interestingly, the levels of these two compounds in nuclei were much greater than in the soluble cytoplasmic/vacuolar fraction, whereas the more abundant glycosides of formononetin and medicarpin were found in the soluble/vacuolar fraction but not at all in the nuclei (SI Fig. 14), consistent with their previously reported vacuolar localization (25).

Discussion

M. truncatula cell suspension cultures exhibit very different qualitative, quantitative, and temporal responses to YE and MJ (13). However, in the present cell culture line, both treatments induced medicarpin production. The overall response to YE was characterized by a massive accumulation of transcripts encoding nearly all of the currently identified genes annotated as encoding the enzymes that function in isoflavonoid biosynthesis upstream of formononetin, including enzymes of the shikimate pathway that provide phenylalanine as precursor. Most of these annotations are based on sequence identity alone, although several are experimentally supported for *M. truncatula* or orthologs in *Medicago sativa* (20, 26, 27). The annotations of those few members of the above gene families associated with reactions downstream of formononetin that are seen to be induced by MJ in Fig. 1 are potentially suspect; for example, the products of 4CL-like genes may not use 4-coumarate as substrate (28, 29). Likewise, of those genes upstream of formononetin that are not induced by MJ, recombinant TC100787 does not possess isoflavone 2′-hydroxylase activity despite its annotation (30), and not all isoflavone reductase (IFR)-like genes encode proteins with IFR activity (31).

The fact that most of the early flavonoid pathway genes were not induced (and in several cases were repressed) by MJ supports a novel genetic mechanism controlling precursor supply for MJ-induced medicarpin accumulation, featuring uncoupling of induction of the early and late branches of the pathway and provision of precursors for the late reactions by mobilization of preformed intermediates. The differential expression of transcription factor genes in response to YE or MJ in *Medicago* cell cultures provides a likely basis for this phenomenon.

Despite the concept that phytoalexins are derived from distant precursors through *de novo* synthesis (4), previous studies (25) have suggested that preformed glycosides may represent a precursor pool for phytoalexin biosynthesis. Such isoflavone mobilization into medicarpin was more pronounced if flux into the pathway was blocked by application of the PAL inhibitor L-α-aminooxy-β-phenylpropionic acid in chickpea and alfalfa cell cultures (25, 32, 33). The nature of the signaling mechanism that senses flux through the phenylpropanoid and isoflavonoid pathways and translates this sensing into mobilization of vacuolar contents remains to be determined. MJ itself cannot be ruled out as a candidate.

The rapid induction of β-glucosidases by MJ paralleled the rapid response of medicarpin biosynthetic genes to YE. Three of the MJ-induced β-glucosidases were active with formononetin glucoside and therefore candidates for involvement in precursor mobilization for medicarpin biosynthesis. G2 preferred isoflavonoid over flavonoid glucosides, and G4, with a broad substrate preference, was down-regulated by YE. Other β-glucosidases have been shown to exhibit preference for specific (iso)flavonoid compounds, such as a set of chickpea isoenzymes possessing K_m values for isoflavones of at least 100-fold lower than for other phenolic glycosides (34), enzymes from white lupin roots that, like the *Medicago* enzymes, can cleave isoflavone glucosides but not kaempferol 3-*O*-β-glucoside (35), and an enzyme from soybean roots (GmICHG) that has very high specificity and turnover for gensitein and daidzein malonyl glucosides (36). This enzyme is found in the cell wall fraction in soybean roots, and, of the *Medicago* enzymes reported here, is most closely related to G2 (70% at the amino acid level) (SI Fig. 12). Based on either confocal microscopy or computational prediction, G2, G3, and G4 are localized to either vacuole or cytosol. The isoflavone conjugates of chickpea cell suspension cultures are vacuolar localized (37), and these compounds were found in the soluble fraction (cytoplasmic plus vacuolar contents) in *Medicago*. Cell fractionation studies suggested that chickpea isoflavone glucosidase activity was primarily cytoplasmic, whereas the malonylesterase activity responsible for the initial degradation of isoflavone-7-*O*-glucoside-6″-malonate (38) was associated with the vacuolar membrane (37). This type of enzyme has yet to be characterized at the molecular level.

MJ induced transcription of a set of ABC transporters, one or more of which might potentially function in transport of isoflavones or isoflavone glycosides from vacuole to cytosol. However, although it is believed that vacuolar transport of acylated anthocyanins is mediated by ABC transporters, the role of these proteins in the vacuolar transport of most other phenylpropanoid-derived natural products remains unclear, and it is generally assumed that these ATP-requiring transporters function to move compounds from the cytosol where ATP concentrations are high, rather than from the apoplastic or vacuolar compartments (39). Other transporter types, such as members of the MATE family, also act to transport natural products into, rather than out of, the vacuole (40). Interestingly, although YE induced secretion of polyphenolic metabolites from the *Medicago* cell cultures to the culture medium, MJ did not (M.A.F., R.A.D., and L.W.S., unpublished data), despite the induction of many ABC transporter genes. Further studies are required to determine whether any of these, or other MJ-induced transporters, play a role in isoflavone mobilization or sequestration, the nature of their substrates *in vivo*, and the subcellular sites of their action.

The exclusive localization of G1 to nuclei was surprising, although free or substituted flavanols or flavonols have been localized to plant nuclei (41–43), and CHS and CHI localize to nuclei in several different cell types of *Arabidopsis* (44). The significance of the almost exclusive presence of coumestrol and 4′,7-dihydroxyflavone aglycones in *Medicago* root nuclei is likewise not yet clear. G1 was the most highly expressed of the MJ-induced glucosidases; reverse genetic studies might reveal whether it plays a metabolic or regulatory role during the MJ-induced response.

A number of plant natural products, such as the cyanogenic glycosides (45), exist as inactive conjugates that are activated by hydrolysis of glycosidic bonds after physical damage to the cells. It is generally assumed that release of these compounds arises from mixing of substrate with previously sequestered glycosidases due to physical rupture of the vacuolar membrane. Our results indicate that the wound signal MJ induces *de novo* synthesis of glycosidases, facilitating release of prestored intermediates for the biosynthesis of defensive compounds (Fig. 5). On the basis of its *in vitro* activity, probable subcellular localization, and similarity to soybean isoflavone glucosidase, G2 is the most likely candidate for involvement in turnover of formononetin glucoside during wound signal-induced medicarpin synthesis in *M. truncatula*.

Materials and Methods

Plant Material. Cell suspension cultures were initiated via callus from roots of *M. truncatula* Gaerth Jemalong (line A17), main-

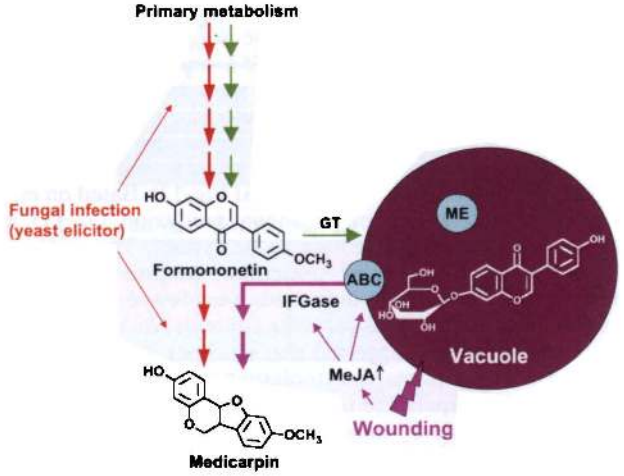

Fig. 5. Model showing the different biochemical and genetic mechanisms for the induction of medicarpin by pathogen and wound signals. In the absence of elicitation, the cells gradually accumulate constitutive isoflavone glucosides and malonyl glucosides in the vacuole (green arrows). After exposure to the pathogen mimic YE, the pterocarpan phytoalexin medicarpin is synthesized *de novo* from L-phenylalanine and malonyl CoA (primary metabolism) (red arrows). Wounding induces MJ accumulation, which acts as a signal for transcriptional activation of isoflavone-specific β-glucosidases that localize to the vacuole and/or cytosol, where they convert conjugates to free isoflavones. The glycosides or aglycones may exit the vacuole via MJ-induced transporters (ABC transporters are shown, although the few studied to date operate in the opposite direction). This process may be initiated by removal of malonyl groups from the sugar unit of the isoflavone conjugates via a specific malonylesterase (ME). MJ induces the downstream enzymes of medicarpin biosynthesis (purple arrows), resulting in medicarpin production at the expense of preformed intermediates.

tained in a modified Schenk and Hildebrandt medium (46), and subcultured every 10–14 days. Growth and elicitation of cell suspension cultures with YE or MJ was performed as described (13, 19). Cells for oligo array analysis were harvested at 21 time points over a total of 48 h. All treatments and time points were represented by triplicate biological samples (i.e., culture flasks). Two- and 24-h elicited and control samples from the same time course were used for Affymetrix array analysis. Metabolite analyses were performed on cells from the passage before that used for transcript analysis; the pattern and timing of metabolite changes was very similar between the two passages (M.A.F., R.A.D., and L.W.S., unpublished data).

Plants of *M. truncatula* ecotype Jemalong A17 and tobacco ecotype NC Cornell were grown in 4.5-inch diameter pots containing professional blend soil (Sun Gro Horticulture, Bellevue, WA) at a temperature of 20°C/19°C (day/night). Plants were fertilized at time of watering with a commercial fertilizer mix [Peters Professional 20–10–20 (N-P-K) General Purpose, The Scotts Company, Marysville, OH].

Microarray Analysis. Oligonucleotide microarrays representing 16,086 TC sequences, primarily from various *M. truncatula* EST sequencing projects (http://compbio.dfci.harvard.edu/tgi/cgi-bin/tgi/gimain.pl?gudb = medicago) have been described (13, 15). A reference design was used in which all RNA samples for both control and elicited cells were compared with RNA from a separate batch of nonelicited cells. Three biological replicates were used. The Affymetrix GeneChip *Medicago* Genome Array (Affymetrix, Santa Clara, CA), containing 61,200 *Medicago* probe sets, was also used for microarray analysis. RNA samples were prepared from cells exposed to YE or MJ for 2 or 24 h, along with the corresponding unelicited controls. Two biological replicates were used for minimal statistical treatment, and mean values for each treatment were divided by the corresponding control baseline values.

Isolation of RNA, hybridization of arrays, statistical analysis, and confirmation of results by RT-PCR are described in *SI Text*. Primers for use in RT-PCR are listed in SI Table 8.

Cloning, Expression, and Purification of *M. truncatula* β-Glucosidases. Full-length cDNA clones representing G1 (GenBank accession no. AW584653), G2 (GenBank accession no. AW684618), G3 (GenBank accession no. CX531312), and G4 (GenBank accession no. AW586688) were confirmed by sequencing. They were then cloned by PCR into pPICZA (G1, G4), pPICZαA (G2), or pPICZαC (G3) expression vectors (Invitrogen, Carlsbad, CA) using primers (SI Table 9) to introduce EcoRI/ApaI sites for G1 and G4 and EcoRI/SacII sites for G2 and ClaI/SacII sites for G3. All β-glucosidases were expressed as translational fusions carrying C-terminal hexa-histidine tags. Vectors carrying insertions were digested with SacI and transformed into *P. pastoris* X-33 cells. Individual colonies were cultured at 30°C overnight in BMGY medium, and expression was then induced in BMMY medium according to the EasySelect Pichia Expression kit manual (Invitrogen). Cultures were centrifuged, and pellets (G1 and G4) were resuspended in extraction buffer (50 mM sodium phosphate, pH 7.4/1 mM PMSF/1 mM EDTA/5% glycerol). Cells were disrupted by vortexing eight times with an equal volume of acid-washed glass beads (size 0.5 mm; Sigma-Aldrich, St. Louis, MO) and centrifuged, and the resulting supernatant was collected and used for purification of G1 or direct assay of G4. G2 and G3 were secreted into the medium, which was centrifuged, and concentrated 100-fold by using Amicon Ultra-15 centrifugal filter devices and Ultracel-30 k membranes (Millipore, Billerica, MA). Media concentrate was used for purification for G2 or direct assay of G3. G1 and G2 were purified with the MagneHis protein purification system kit (Promega, Milwaukee, WI).

Kinetic Analysis of β-Glucosidases. Standard assay of β-glucosidase activity is described in *SI Text*. For kinetic studies with G1 and G2, the rate of substrate hydrolysis was measured at 30°C by monitoring the continuous release of *p*-nitrophenol from pNPG at 400 nm with a DU800 spectrophotometer (Beckman Coulter, Fullerton, CA). Two micrograms of purified G1 or 1 μg of purified G2 was added to reaction mixtures containing 100 mM citrate-phosphate buffer (pH 5.2) and 0–10 mM pNPG for G43298, or 0–1.5 mM pNPG for G2, in a total volume of 100 μl.

Reactions with ononin, genistin, and apigenin-7-*O*-glucoside (0–250 μM) were performed at 30°C in 50-μl volumes containing 1 μg of purified G1 or 0.5 μg of G2 and 100 mM citrate-phosphate buffer (pH 5.2) and stopped with trichloroacetic acid after 15-min incubation for G1 or 10 min for G2. Reactions were extracted with 250 μl of ethyl acetate, and 225 μl of the organic fraction was dried under N_2, resuspended in methanol, and analyzed by HPLC as described (47). K_m and K_{cat} values were calculated by fitting the initial velocity data to Lineweaver–Burk double reciprocal plots.

3D Homology Modeling of *M. truncatula* G43298. The amino acid sequence of *M. truncatula* G1 was used to search the Protein Data Bank, in which cyanogenic β-glucosidase from white clover (*T. repens*) (ID no. 1CBG) was closest to G1, with 55.6% identity at the amino acid sequence level. The amino acid sequences of G1 and white clover β-glucosidases were realigned by using the Clustal W (1.82) method, and, subsequently, homology was modeled by using the program Modeler (48) with the structural coordinates retrieved from the protein database. Five models were generated and ranked by Model Rank bundled in the Modeler package. The top-ranked model was chosen and visualized under O (49).

HPLC/MS Analysis. Extraction of phenolic compounds from cell suspension cultures and LC-MS analysis were performed as described (14).

***In Planta* Transient Expression and Confocal Microscopy.** Construction of β-glucosidase-EGFP fusions for particle bombardment or agro-infiltration is described in *SI Text*. One tobacco leaf or three detached *M. truncatula* A17 leaves were separated and distributed in the center of Petri dishes on wet filter paper. *M. truncatula* cell suspension cultures were filtered and placed in the Petri dish on 1% agarose. Particle bombardment with gold particles coated with plasmid DNA was performed as described (47). The gene constructs were delivered into the plant tissues at a pressure of 650 or 1,100 p.s.i. for tobacco leaf or *M. truncatula* leaves and cells, respectively. Agro-infiltration is described in *SI Text*.

Images were collected by using a TCS SP2 AOBS laser scanning confocal microscope (Leica, Manheim, Germany). EGFP was excited at 488 nm, and the emission window was set at 500–554 nm. Single focal plane EGFP images and Z-series images were composed of four integrated frames each, and Z-series were projected by using the maximum projection tool of the Leica confocal software. Autofluorescence of chloroplasts was imaged by using excitation at 568 nm and an emission window from 550 to 700 nm.

We thank Drs. Rujin Chen and Li Tian for critical reading of the manuscript, Dr Michael Udvardi for sharing *Medicago* gene atlas data, and Dr Aline Valster for assistance with confocal microscopy. This work was supported by National Science Foundation Plant Genome Program Research Award DBI-0109732, National Science Foundation Equipment Grant DBI-0400580, and the Samuel Roberts Noble Foundation. C.-J.L. was supported by the Laboratory Directed Research Program of Brookhaven National Laboratory under contract with the Department of Energy and the Plant Feedstock Genomics for Bioenergy program from the Office of Biological and Environmental Research of the Department of Energy.

1. Hain R, Reif HJ, Krause E, Langebartels R, Kindl H, Vornam B, Weiese W, Schmelzer E, Schrier PH, Stocker RH, Stenzel K (1993) *Nature* 361:153–156.
2. Essenberg M (2001) *Physiol Mol Plant Pathol* 59:71–81.
3. Papadopoulou K, Melton RE, Leggett M, Daniels MJ, Osbourn AE (1999) *Proc Natl Acad Sci USA* 96:12923–12928.
4. VanEtten H, Mansfield JW, Bailey JA, Farmer EE (1994) *Plant Cell* 6:1191–1192.
5. Kawalleck P, Plesch G, Hahlbrock K, Somssich IE (1992) *Proc Natl Acad Sci USA* 89:4713–4717.
6. Dixon RA (2001) *Nature* 411:843–847.
7. Chappell J, VonLanken C, Vögeli U (1991) *Plant Physiol* 97:693–698.
8. Sallaud C, Zuanazzi J, El-Turk J, Leymarie J, Breda C, Buffard D, de Kozak I, Ratet P, Husson P, Kondorosi A, Esnault R (1997) *Mol Plant–Microbe Interact* 10:257–267.
9. Lane GA, Sutherland ORW, Skipp RA (1987) *J Chem Ecol* 13:771–783.
10. Russell GB, Sutherland ORW, Hutchins RFN, Christmas PE (1978) *J Chem Ecol* 4:571–579.
11. Tava A, Odoardi M (1996) in *Saponins Used in Food and Agriculture*, eds Waller GR, Yamasaki T (Plenum, New York), pp 97–109.
12. Achnine L, Huhman DV, Farag MA, Sumner LW, Blount JW, Dixon RA (2005) *Plant J* 41:875–887.
13. Suzuki H, Reddy MSS, Naoumkina M, Aziz N, May GD, Huhman DV, Sumner LW, Blount JW, Mendes P, Dixon RA (2005) *Planta* 220:698–707.
14. Farag MA, Huhman DV, Lei Z, Sumner LW (2006) *Phytochemistry* 68:342–354.
15. Aziz N, Paiva NL, May GD, Dixon RA (2005) *Planta* 221:28–38.
16. Chen CC, Shieh B, Jin YT, Liau YE, Huang CH, Liou JT, Wu LW, Huang WY, Young KC, Lai MD, *et al.* (2001) *J Biomed Sci* 8:214–222.
17. Akashi T, Sawada Y, Shimada N, Sakurai N, Aoki T, Ayabe S (2003) *Plant Cell Physiol* 44:103–112.
18. Akashi T, Aoki T, Ayabe S (2005) *Plant Physiol* 137:882–891.
19. Broeckling CD, Huhman DV, Farag M, Smith JT, May GD, Mendes P, Dixon RA, Sumner LW (2005) *J Exp Bot* 56:323–336.
20. Deavours BE, Dixon RA (2005) *Plant Physiol* 138:2245–2259.
21. Barrett T, Suresh CG, Tolley SP, Dodson EJ, Hughes MA (1995) *Structure (London)* 3:951–960.
22. Zeidler M, Zhou Q, Sarda X, Yau VP, Chua NH (2004) *Plant J* 40:355–365.
23. Cokol M, Nair R, Rost B (2000) *EMBO Rep* 1:411–415.
24. Rout MP, Aitchison JD (2001) *J Biol Chem* 276:16593–16596.
25. Mackenbrock U, Gunia W, Barz W (1993) *J Plant Physiol* 142:385–391.
26. Gowri G, Paiva NL, Dixon RA (1991) *Plant Mol Biol* 17:415–429.
27. McKhann HI, Hirsch AM (1994) *Plant Mol Biol* 24:767–777.
28. Cukovic D, Ehlting J, VanZiffle J, Douglas CJ (2001) *Biol Chem* 382:645–654.
29. Costa MA, Bedgar DL, Moinuddin SGA, Kim K-W, Cardenas CL, Cochrane FC, Shockey JM, Helms GL, Amakura Y, Takahashi H, *et al.* (2005) *Phytochemistry* 66:2072–2091.
30. Liu CJ, Huhman DV, Sumner LW, Dixon RA (2003) *Plant J* 36:471–484.
31. Gang DR, Kasahara H, Xia ZQ, Mijnsbrugge KV, Bauw G, Boerjan W, Van Montagu M, Davin LB, Lewis NG (1999) *J Biol Chem* 274:7516–7527.
32. Mackenbrock U, Barz W (1991) *Z Naturforsch* 46:43–50.
33. Kessmann H, Edwards R, Geno P, Dixon RA (1990) *Plant Physiol* 94:227–232.
34. Hösel W, Barz W (1975) *Eur J Biochem* 57:607–616.
35. Pislewska M, Bednarek P, Stobiecki M, Zielisska M, Wojtaszek P (2002) *Plant Cell Environ* 25:20–40.
36. Suzuki H, Takahashi S, Watanabe R, Fukushima Y, Fujita N, Noguchi A, Yokoyama R, Nishitani K, Nishino T, Nakayama T (2006) *J Biol Chem* 281:30251–30259.
37. Mackenbrock U, Vogelsang R, Barz W (1992) *Z Naturforsch* 47:815–822.
38. Hinderer W, Köster J, Barz W (1986) *Arch Biochem Biophys* 248:570–578.
39. Martinoia E, Maeshima M, Neuhaus HE (2007) *J Exp Bot* 58:83–102.
40. Marinova K, Pourcel L, Weder B, Schwarz M, Barron D, Routaboul J, Debeaujon I, Klein M (2007) *Plant Cell* 19:2023–2038.
41. Feucht W, Treutter D, Polster J (2004) *Plant Cell Rep* 22:430–436.
42. Peer WA, Brown DE, Tague BW, Muday GK, Taiz L, Murphy AS (2001) *Plant Physiol* 126:536–548.
43. Hutzler P, Fischbach R, Heller W, Jungblut TP, Reuber S, Schmitz R, Veit M, Weissenböck G, Schnitzler JP (1998) *J Exp Bot* 49:953–965.
44. Saslowsky DE, Warek U, Winkel BSJ (2005) *J Biol Chem* 280:23735–23740.
45. Zagrobelny M, Bak S, Rasmussen AV, Jørgensen B, Naumann CM, Møller BL (2004) *Phytochemistry* 65:293–306.
46. Dixon RA, Dey PM, Murphy DL, Whitehead IM (1981) *Planta* 151:272–280.
47. Liu CJ, Dixon RA (2001) *Plant Cell* 13:2643–2658.
48. Marti-Renom MA, Stuart AC, Fiser A, Sanchez R, Melo F, Sali A (2000) *Annu Rev Biophys Biomol Struct* 29:291–325.
49. Jones TA, Zou JY, Cowan SW, Kjeldgaard M (1993) *Acta Crystallogr D* 49:148–157.